Enhanced Power from Chambered Benthic Microbial Fuel Cells

ARTICLE *in* ENVIRONMENTAL SCIENCE AND TECHNOLOGY · DECEMBER 2007

Impact Factor: 5.33 · DOI: 10.1021/es071740b · Source: PubMed

3 AUTHORS, INCLUDING:

Clare Reimers
Oregon State University
88 PUBLICATIONS **4,740** CITATIONS

SEE PROFILE

Enhanced Power from Chambered Benthic Microbial Fuel Cells

MARK E. NIELSEN,*,† CLARE E. REIMERS,† AND HILMAR A. STECHER, III†,‡

Hatfield Marine Science Center and College of Oceanic and Atmospheric Sciences, Oregon State University, Newport Oregon 97365

We describe a new chamber-based benthic microbial fuel cell (BMFC) that incorporates a suspended, high surface area and semi-enclosed anode to improve performance. In Yaquina Bay, OR, two chambered BMFC prototypes generated current continuously for over 200 days. One BMFC was pumped intermittently, which produced power densities more than an order of magnitude greater than those achieved by previous BMFCs with single buried graphite-plate anodes. On average, the continuous power densities with pumping were 233 mW/m^2 (2.3 W/m^3); peak values were 380 mW/m^2 (3.8 W/m^3), and performance improved over the time of the deployments. Without pumping, high power densities could similarly be achieved after either BMFC was allowed to rest at open circuit. A third chambered BMFC with a 0.4 m^2 footprint was deployed at a cold seep in Monterey Canyon, CA to test the new design in an environment with natural advection. The power density increased 5-fold (140 mW/m^2 vs 28 mW/m^2) when low-pressure check valves allowed unidirectional flow through the chamber.

Introduction

Benthic microbial fuel cells (BMFCs) generate electricity from the electropotential difference between oxic seawater and anoxic sediments (*1*−*4*). Electrons are delivered to the anode by microorganisms either directly from organic material or indirectly from inorganic products of organic matter degradation (*5*). At the cathode, these electrons reduce dissolved oxygen to form water. Since microorganisms cause organic matter oxidation in natural anoxic environments to proceed through a variety of interactive electron acceptors (*6*, *7*), the processes at the anode can be especially complex and critical to BMFC performance.

In general, BMFCs produce relatively low levels of power due to low rates of diffusion in sediments, low concentrations of labile organic matter, and passivation of anode surfaces (*2*−*4*, *8*−*12*). Among strategies attempted to increase power from BMFCs, the most successful have been (i) employing carbon cloth anodes enriched with organic substrates (*13*) and (ii) using a rotating cathode (*9*). There have also been many improvements in the technology of wastewater-fueled MFCs that have been associated with pumping waste fluids through porous anode materials contained in chambers (*14*−*18*). Guided by these advances, we hypothesized that power generation from BMFCs could be increased further by removing the anode from the sediments and enclosing it in a benthic chamber. Incorporating the benthic chamber would enable the use of high surface area anodes and the advection of reductant-rich porewater to anode materials.

As BMFCs are intended to operate as long-term power sources in aquatic environments, the most relevant evaluation procedure is to conduct an extended discharge experiment under field conditions with some program of controlled cell potential (E_{cell}), current (I), or external load resistance(s) (R_{ext}). The system can be represented by using Ohm's law ($E_{cell} = IR_{ext}$), and internal resistance terms may be assigned to each of the processes that cause a drop in potential from the open circuit voltage ($E_{cell} = OCV - IR_{int}$ (*19*)). As described by Logan et al. (*19*), the three main loss categories that contribute to the steady-state internal resistance (R_{int}) are ohmic losses (R_o), activation losses (R_a), and mass-transfer losses (R_{mt}); giving the relationship

$$R_{int} = R_o + R_a + R_{mt} \quad (1)$$

R_o includes resistances to the flow of current through connections in the device and the resistance to counter-ion flow through the electrolyte, which is seawater in ocean BMFCs (there are no proton exchange membranes). R_a refers to losses due to the activation energy required by oxidation/reduction reactions. R_{mt} are losses that arise from limitations in the rate of delivery of electroactive species to the electrodes. The rate of delivery is controlled by the concentration of electroactive species in the vicinity of the electrodes and by factors that determine mass transport. The terms R_a and R_{mt} may also be separated into anode and cathode components and will vary depending on the load placed on the system (*19*).

In this paper, we present the results from two versions of chambered BMFCs developed to address the limitation of slow diffusion in sediment MFCs. We use field data to estimate the magnitude of the various loss terms, and we show that the new design of BMFC avoids the negative effects of anode passivation that have been previously observed in sediment microbial fuel cells.

Experimental Procedures

Yaquina Bay BMFCs. The first version of a chambered BMFC was constructed in duplicate and evaluated in Yaquina Bay, OR (latitude 44°,37.47′, longitude 124°,02.60′) at a site where the average water depth was approximately 6 m with tidal height variations of up to 3 m. These BMFCs (Figure 1a) differed from previous designs in three important ways: (i) the anode was enclosed in a benthic chamber and not buried in the sediments, (ii) high surface area carbon fiber brush electrodes (*20*) were used for the anodes as well as the cathodes, and (iii) the cathodes were twice as long as the anodes (2 m vs 1 m). The electrodes were taken from a commercially available seawater battery (SWB 1200; Kongsberg Maritime AS, Norway). They consisted of fine carbon fibers densely packed on twisted-pair titanium wires and had a manufacturer reported surface area of 26.3 m^2 per meter of electrode. Similar carbon brush anodes were investigated in small laboratory MFCs by Logan et al. (*21*). The BMFC chambers were fabricated from hollow acrylic cylinders with an open bottom and gasket-sealed lid (0.02 m^2 cross-sectional area, 48 cm height). Divers pushed the two chambers into the sediment, 2 m apart, with the bottoms of the cylinders approximately 38 cm below the sediment−water interface, resulting in an anode chamber

* Corresponding author e-mail: mnielsen@coas.oregonstate.edu.
† Oregon State University.
‡ Current address: U.S. Environmental Protection Agency, Pacific Coastal Ecology Branch, Newport, OR 97365.

10.1021/es071740b CCC: $37.00
Published on Web 10/17/2007

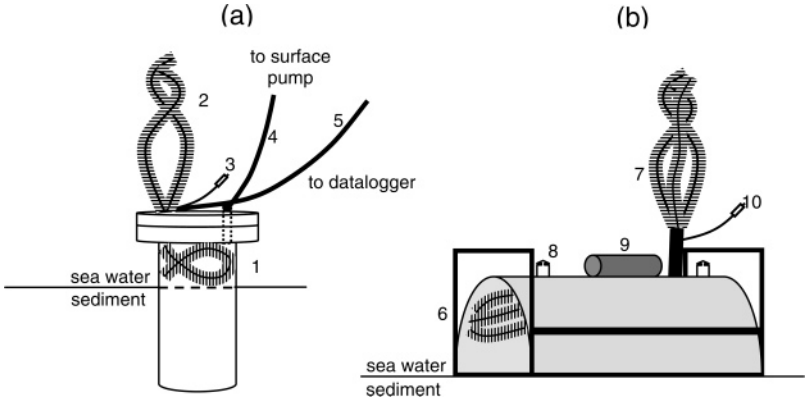

FIGURE 1. (a) Schematic of the Yaquina Bay BMFCs. Each BMFC included a 1 m long carbon brush anode inside an anode chamber with a 2×10^{-3} m^3 volume (1); a 2 m long carbon brush cathode (2); a reference electrode (3); and a sampling tube fitted to a port (4). Electrodes were connected to the data logger through 20 m of 12-gauge, 3-conductor wire (5). (B) Monterey BMFC was constructed from a piece of plastic sewer pipe and included a 3 m long carbon brush anode (6); a 4 m long carbon brush cathode (7); two identical check valves (8); a titanium pressure housing containing passive potentiostat and dataloggers (9); and a reference electrode (10).

volume above the sediment of approximately 2×10^{-3} m^3. Each lid was equipped with a quick-connect port that allowed fluids from inside the chamber to be sampled. Samples were collected by pumping chamber fluids through 20 m of 0.43 cm (i.d.) low-density polyethylene tubing.

The whole-cell potential (E_{cell}), anode potential (E_{an}), and current (I) of the BMFCs were measured with a multi-channel data logger (Agilent Technologies, Santa Clara, CA). E_{an} was measured versus a Ag/AgCl/seawater reference electrode mounted on the outside of the chamber lid. At an average temperature of 11.8 °C, an estimated chloride activity of 320 mmol/kg, and E_o = 222 mV, we calculated that the reference electrode had an average potential of 248 mV versus SHE. The cathode potential (E_{cath}) was calculated from the measured E_{cell} and E_{an}. The electrodes were connected to the data logger through 20 m of 12-gauge, 3-conductor cable (WireXpress, Riverside, CA) with underwater pluggable connectors (Impulse, San Diego, CA). The power is the product of E_{cell} and I and is reported as power density, normalized to the seafloor area or anode chamber volume above the sediment since these parameters are germane to practical applications of this technology.

The Yaquina Bay field evaluations included a long-term discharge experiment with intermittent pumping and sampling and a set of polarization experiments. During the former, each circuit included a passive potentiostat (North-West Metasystems, Bainbridge Island, WA) set so that no current would flow at E_{cell} <0.5 V but the circuit would pass as much current as needed to maintain a 0.5 V difference between anode and cathode. No additional external resistance was applied since the potentiostat automatically controls R_{ext} to maintain the set potential. During the polarization experiments, an adjustable resistor was used in place of the passive potentiostat, and R_{ext} was varied manually.

Long-Term Discharge Experiment. After deployment, the Yaquina Bay BMFCs (denoted A and B) were left at open circuit until potentials were fully developed and stable (E_{cell} ≈ 0.8V). Then, on what is designated as day 0, the long-term discharge of both BMFCs was initiated, and cell parameters were monitored under identical conditions except that BMFC A was pumped only to collect two samples (one on day 0 prior to closing the circuits and the other on day 15, with 20 min of pumping required for each sample), whereas BMFC B was pumped for several prolonged time periods to enable slow advection of sediment porewater into the anode chamber. The three principal pumping periods were days 15−17, days 35−51, and days 153−200. During pumping periods, withdrawal rates were measured volumetrically and maintained at 6.3 mL/min (5×10^{-6} m/s across the sediment−water interface) whenever the pump was turned on. The residence time of fluid within the anode chamber under these conditions was 5.3 h.

Chemical Methods. Water samples for chemical analyses were collected during pumping directly from the polyethylene tubing into 50 mL glass syringes, thus avoiding contact with oxygen. The syringes were transferred to the laboratory where subsamples for various analyses were expelled. Dissolved organic carbon (DOC) subsamples were collected first and filtered through pre-combusted glass microfiber filters (GF/F). Then, the syringe and remaining sample were transferred into an anaerobic nitrogen atmosphere within a glove bag where the sample water was filtered through a 0.45 μm syringe filter (Pall, Ann Arbor, MI) and partitioned for dissolved inorganic carbon (DIC), sulfide, ammonia, sulfate, and chloride analyses.

Total sulfide and ammonia were measured spectrophotometrically (*22*, *23*). Sulfate and chloride were measured after a 500-fold dilution by ion chromatography (DX-500 with an AS-12 column, Dionex, Sunnyvale, CA). DOC samples were preserved with H_3PO_4 and analyzed on a TOC−V_{CSH} analyzer (Shimadzu Scientific Instruments, Columbia, MD). DIC samples were fixed with saturated $HgCl_2$ and analyzed coulometrically (*24*).

Polarization Experiments. Two polarization experiments were conducted with each BMFC in Yaquina Bay (275−285 days post-deployment), one with the pump off and one with the pump on. Beginning with the cell at a fully stabilized open circuit potential, the circuit was closed, and the external resistance was stepped through 12 resistance values from 1000 to 5 Ω, and E_{cell} and I were measured for 15 min at each step. Pseudo-steady-state cell potentials and currents were estimated by averaging measurements over the last minute of each step (10 s interval).

Monterey Canyon BMFC. To test the chamber design in an environment with natural advection, we built a second, larger, chambered BMFC and deployed it at a methane cold seep at a water depth of 960 m in Monterey Canyon off the coast of central California (latitude 36°,46.57′, longitude 122°,-05.15′). This chamber was constructed from a 66 cm long piece of 60 cm plastic sewer pipe cut lengthwise, giving a volume of approximately 2.0×10^{-2} m^3 and a footprint of 0.4 m^2 (Figure 1b). The Monterey BMFC included 3 m of carbon brush anode suspended above the sediment within the chamber and 4 m of carbon brush cathode (*20*) connected to the outside and suspended above the seafloor with a syntactic foam float. E_{cell} and E_{an} were measured directly, and I was converted to a voltage and recorded with dataloggers (Volt101, Madgetech, Warner, NH). E_{an} was

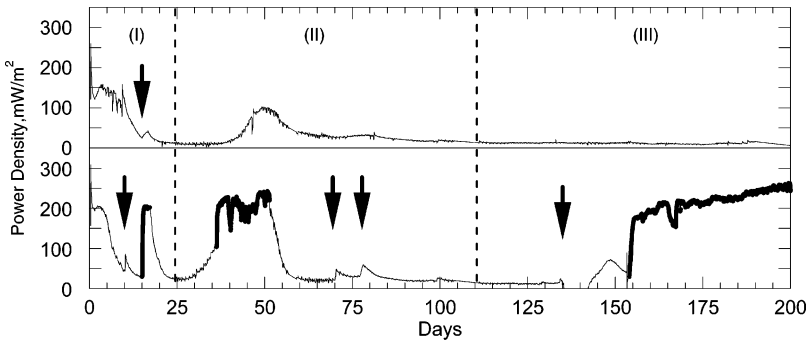

FIGURE 2. Power density from Yaquina BMFCs A (upper panel) and B (lower panel) from the long-term discharge experiment. Prolonged pumping periods are indicated by the bold sections on the record of BMFC B. Arrows represent short-duration pumping for sampling or response testing.

measured versus a Ag/AgCl/seawater reference electrode. E_{cell} was controlled using a passive potentiostat as described previously with the voltage set at 0.4 V. The BMFC was equipped with check valves, allowing unidirectional flow out of the chamber but no mechanical pumps. The BMFC was deployed and recovered by a remotely operated submersible vehicle (ROV) operated by the Monterey Bay Aquarium Research Institute. It was initially deployed for 68 days and then recovered, at which time the check valves were changed and then the chamber was redeployed at the same location. The ROV has a navigational ability that allowed us to replace the BMFC on the same footprint (±0.1 m) when it was redeployed. In the first deployment, the valves were spring-loaded piston check valves with a nominal cracking pressure of 0.5 psi. In the second deployment, the valves were swing check valves with a cracking pressure of 0.1 psi.

Results and Discussion

Evolution of Power Generation. Before the long-term discharge, the Yaquina BMFCs were at open circuit for several weeks. During this time, sulfate reduction in the anode chambers led to HS^- concentrations that were determined to be 5.7 and 4.1 mM, in BMFC A and B, respectively, just before their circuits were closed. After the circuits were closed, power generation proceeded in three phases (Figure 2). Phase I was characterized by high power resulting from electrochemical oxidation of the accumulated sulfide, and it presumably resulted in the deposition of elemental sulfur at the anode. The primary feature of Phase II was a secondary power maximum peaking in BMFC A at 100 mW/m^2 (1 W/m^3) on day 50 but partially obscured in the record of BMFC B due to pumping effects. We hypothesize that the secondary peak may have arisen because of the enrichment of microbes that can disproportionate sulfur and/or produce other previously unavailable electron donors. Similarly, a microbial succession in a laboratory MFC was described by Aelterman et al. (*25*), which was correlated to improved performance and the possible production of electron-transfer mediators. More experiments are needed to test this hypothesis in chambered BMFCs, but previous experiments in Yaquina Bay showed enrichments of *Desulfobulbus, Desulfocapsa*, and *Cytophagales* groups on buried anodes after 6 months of current generation (*10*). We have observed secondary peaks in other MFC experiments, indicating that environmental forcing such as changes in temperature, salinity, or tidal fluctuations specific to this experiment were not the cause. We also note that the onset of the Phase II peak occurred earlier in BMFC B, which had been pumped (and thus passed more cumulative charge). In Phase III, the power densities of both cells when unpumped were steady and averaged about 13 mW/m^2 (0.1 W/m^3). Apparently, this power density represents the long-term energy available if anode reactants are supplied to the anode chamber from this sediment by diffusion and occasional bioirrigation. An exception was days 135−142 in BMFC B when E_{cell} temporarily dipped below 0.5 V so no current was passed.

Effect of Pumping on R_{mt}. For the Yaquina Bay fuel cells, pumping led to approximately a 15-fold increase in sustainable power density. The effective R_{int} of an unpumped BMFC at steady-state was approximately 577 Ω ((0.8−0.5 V)/0.52 mA), and when pumped, R_{int} was approximately 38 Ω ((0.8−0.5 V)/7.9 mA). Essentially, advection enhances the mass transfer of anode reactants across the sediment−water interface, and it both dilutes and removes soluble reaction products. By this comparison, the anode mass-transfer resistance, R_{mt}, in the Yaquina Bay BMFCs was at least 93% of the internal resistance when discharged continuously at 0.5 V ((577−38 Ω)/577 Ω). This value supports the observation of Reimers et al. (*3*) that mass transfer to the anode is one of the main limitations of power generation by BMFCs. Furthermore, we used the current interrupt technique (*26*) and determined that both BMFCs had an R_o of 26−30 Ω (corroborated by the polarization experiments presented later). This leaves anodic R_a and any cathode resistance terms as unknowns. These remaining losses, however, were apparently less than ohmic losses, which in turn were dwarfed by anode mass-transfer losses during the long-term discharge of these BMFCs.

We attribute the power increase from pumping to an increase in the concentration of electron donors near the anode rather than to stirring or other hydrodynamic affects. This conclusion was confirmed by a 24 h test during which the BMFC was repeatedly pumped for 1 min and then rested for 29 min. The power density increased smoothly and did not show a specific response to the pumping intervals (Supporting Information Figure S1).

Processes inside the Chamber. Chemical changes (Figure 3) illuminate processes occurring inside the anode chamber. The first sample in each time series represents water in the chamber under unpumped conditions with current being drawn. Subsequent samples reflect an increasing signature of porewater drawn from the sediments underlying the chamber. True porewater chemical concentrations were not observed because the BMFC operated as a chemical reactor and drawing current altered the concentrations of electroactive species in the chamber. Porewater chemistry is also spatially and temporally variable, but representative values from the Yaquina Bay study site were reported by Ryckelynck et al. (*12*). During the days 15−17 pumping interval, the total volume pumped was 18 L or approximately 9 times the anode chamber volume. Assuming an average porosity of 70%, the pumped fluid was drawn from approximately 26 L of sediment.

The data in Figure 3 show a tight coupling between sulfide and power. When the cell was discharged without pumping, sulfide levels were drawn to below measurable concentra-

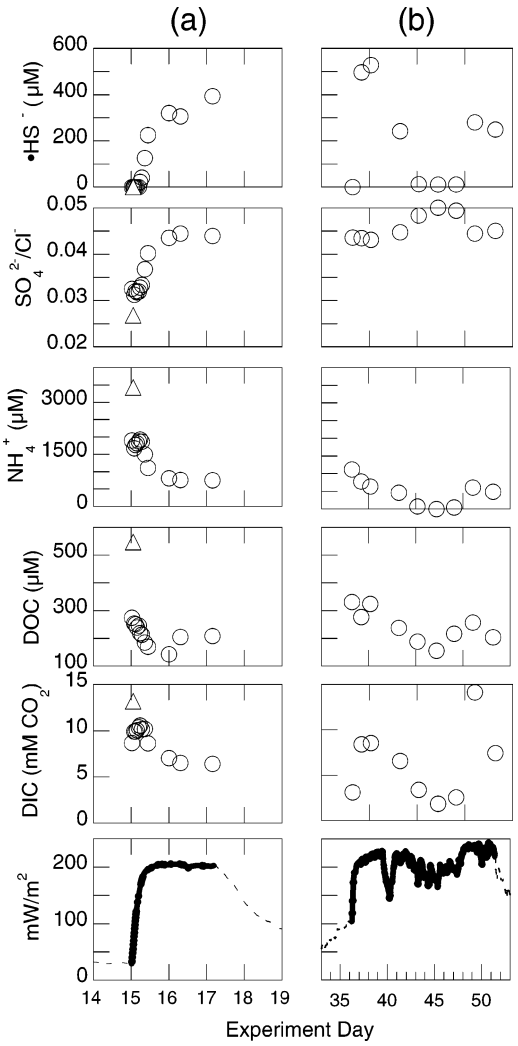

FIGURE 3. Chemistry and power density changes associated with pumping. (a) Results from the first principal pumping period. One water sample was collected for chemical analysis from BMFC A (triangle), and a time series of samples was collected from BMFC B (circles). The pumping period is highlighted in bold in the power density plot (bottom panel). (b) Time series of chemical data over a later extended period of pumping. This pumping period coincided with Phase II of the BMFC evolution so power was increasing even before the onset of pumping (see text for details).

tions. With advection produced by pumping, porewater containing sulfide was drawn from the sediments beneath the BMFC, and there was a concomitant increase in power. On the basis of the time series of sulfate data (normalized to chloride to remove the effects of small salinity variations), sulfate reduction must have been occurring in the chamber since there was more sulfate in the porewater underlying the chamber than within the chamber. This was corroborated by elevated concentrations of DOC, DIC, and ammonia relative to porewater values. Without pumping, the concentration of DOC increased in the anode chamber, suggesting that this organic carbon was in a form not readily oxidized under anaerobic conditions.

During the next pumping period (days 35−51), samples were collected over a longer time period albeit at a lower frequency (Figure 3b). During the period from day 43 to day 47, it appeared that the pump may have been drawing overlying water into the chamber as evidenced by a sulfate/chloride ratio consistent with a background seawater value (0.05 (*27*)) as well as low sulfide and ammonia concentrations. This may have occurred due to the temporary opening of a large burrow(s) by sediment macrofauna in the estuary (*28*). Despite the evidence of overlying water entering the chamber and sulfide dropping below detection, the power production remained relatively high. This is evidence that electrons can be supplied by a tightly coupled sulfur cycle at the anode surface as described previously (*12*, *29*). In addition, the observation of power without measurable sulfide in the bulk chamber fluid could indicate electron donors other than reduced sulfur species.

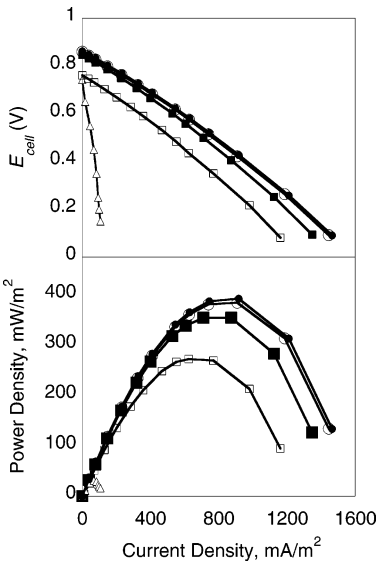

FIGURE 4. Polarization plots of Yaquina BMFC A (squares), BMFC B (circles), and a previous BMFC design (described by Tender et al. (*4*), triangles). Open symbols are without pumping, and solid symbols are with pumping. All polarizations were conducted starting at an open circuit, and then the external resistance was decreased progressively with an adjustable resistor. Peak power densities in BMFCs A and B correspond to external resistances between 20 and 30 Ω.

Polarizations and Comparison to Previous BMFC Designs. We performed polarization experiments with the Yaquina Bay BMFCs to evaluate their peak power characteristics and compare them to previous BMFCs (Figure 4). In the case of BMFC A, pumping the anode chamber for its second polarization caused its open circuit potential to rise to 0.86 V as compared to an initial value of 0.80 V, and then 0.74 V after months without pumping. We speculate the shift from 0.74 to 0.86 V was because the pumping flushed out oxidation products that had accumulated within the chamber during discharge Phases I−III. In contrast, BMFC B was unpumped for only 4 days prior to its second polarization, and during this period, the cell was also off, so no build-up of oxidation products occurred. In all four polarizations, the anode potential showed a significantly larger shift than the cathode potential for each successive step in the polarization. This indicates that these BMFCs were predominantly anode limited (as was intended by a 2:1 ratio of cathode to anode area).

A striking characteristic of all the plots of E_{cell} versus current density (Figure 4) is that they are close to linear, implying a nearly constant R_{int}, which we have calculated as equal to 18−27 Ω by the formulation (OCV − E_{cell})/I. This suggests that under these experimental conditions, R_o was dominant, and the internal resistance was almost entirely dependent upon the resistance of seawater. This is concluded because using a seawater resistivity value of 0.28 Ω m (S = 30, T = 11.8 °C), an electrode spacing distance of 1.5 m, and an area of 0.02 m^2, an independent estimate of the ohmic resistance due to seawater is approximately 21 Ω. Over longer discharge periods than represented by the polarizations, the electron

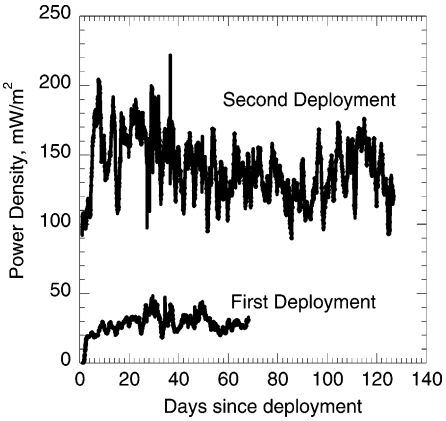

FIGURE 5. Overlay of power density records from two deployments of the Monterey BMFC. At the end of the first deployment, the check valves were changed to a model with a lower cracking pressure and then immediately redeployed. The delay was approximately 6 h due to the transit time for the ROV to surface from 960 m and then return to the seep. During the second deployment, the BMFC began generating current immediately, suggesting that the anodic biofilm survived the trip to the surface.

donors in the anode chamber would be depleted, and the mass-transfer resistance would increase, as evidenced by the high R_{mt} during steady-state discharge from the unpumped chamber.

Polarization curves are one way of comparing different fuel cell designs. In Figure 4, we include polarization data from a previously described BMFC in which the anodes were single graphite plates buried in Yaquina Bay sediment (*4*). The short-term peak power density of the plate anode BMFC was approximately 30 mW/m^2 as compared to 270−380 mW/m^2 (2.7−3.8 W/m^3) for unpumped and pumped chambers, respectively, with the polarizations conducted in the same way for both chambered and buried-plate anode designs. We note, however, that the long-term power densities sustainable by BMFC A (and BMFC B when unpumped) for periods of months were nearly the same as the buried-plate anode BMFC. This suggests a great advantage to operating new chambered designs in a cyclic manner. Similar advantages may be gained with a buried anode, but the high surface area carbon fiber anodes in the chambers are able to discharge at higher current densities than the plate anodes after reactant build-up.

Energy Cost of Pumping. The energy cost of pumping versus the gain in power is an important consideration for the realistic application of chambered designs. As an example, a low-power miniature peristaltic pump (e.g., P625, Instech Laboratories, Plymouth Meeting, PA) requires 225 mW of power for pumping rates up to 7.3 mL/min. This is many times greater than gains of pumping observed in Yaquina Bay (approximately 4.4 mW in terms of actual power for the 0.02 m^2 footprint of these chambers). This energy imbalance may be addressed several ways for full-scale BMFCs. Lower power pumps could be found, pumping rates could be optimized and/or pumps run intermittently, or a pumping system could be developed that does not require any electrical power such as one driven by a vacuum chamber deployed along with the BMFC. Finally, one can design chambers to take advantage of natural processes that may drive porewater advection. These processes include pressure gradients created by waves or flow over sedimentary bedforms (*30*), hydrothermal venting (*31*), and tidally pumped fluid venting at cold seeps (*32*). We tested our second version of a chambered BMFC (Figure 1b) in the latter environment.

Power density records from the two Monterey Canyon deployments are overlaid in Figure 5. The power density from the second deployment was about 5 times greater than from the first deployment. Apparently, the fluid pressure from the seep fell between the cracking pressure of the different valves, so that significant advection into the chamber was only possible with the low-pressure valves. This observation is consistent with the difference in variability between the two records. When a chamber is isolated from advection, one would expect less variability in power generation than a chamber that is open to advection forced by tidal fluctuations or other processes (see Supporting Information Figure S2).

Our group previously deployed BMFCs with buried graphite anodes at a nearby seep (*3*). In that experiment, the maximum power density was 1100 mW/m^2, but that anode was a vertically oriented rod so the anode surface area did not scale with the seafloor footprint. A passivation effect at the anode was also observed, which greatly reduced power over time, and it was attributed to the deposition of elemental sulfur within the pores of the solid graphite anode. The use of carbon fiber anodes inside the chambers showed no electrochemical evidence of power limitation by passivation in either the Yaquina Bay or the Monterey deployments. This may be due to a much higher overall surface area (relative to instrument footprint) and the lack of pores.

Acknowledgments

This work was supported by grants from the Office of Naval Research and the National Science Foundation. We are grateful to Brian Parker, John Buchanan, and Kristina McCann-Grosvenor for their diving assistance and to Joe Jennings and Andrew Ross for analytical help. Discussions with Peter Girguis helped to formulate these experiments, and he coordinated the ROV access. The Monterey deployments were made possible by the expertise of the pilots of the ROV *Ventana* and the crew of the *R/V Pt. Lobos*. This manuscript was improved through helpful conversations with John Westall, Hong Liu, and reviews from several anonymous reviewers.

Supporting Information Available

Figure of results from a 24 h pumping experiment and figure of magnified portion of power density record from the Monterey Canyon BMFC as compared to tide data from Moss Landing, CA. This material is available free of charge via the Internet at http://pubs.acs.org.

Literature Cited

(1) Whitfield, M. The electrochemical characteristics of natural redox cells. *Limnol. Oceanogr.* **1972**, *17*, 383−393.

(2) Reimers, C. E.; Tender, L. M.; Fertig, S.; Wang, W. Harvesting energy from the marine sediment−water interface. *Environ. Sci. Technol.* **2001**, *35*, 192−195.

(3) Reimers, C. E.; Girguis, P.; Stecher, H. A., III; Tender, L. M.; Ryckelynck, N. Microbial fuel cell energy from an ocean cold seep. *Geobiology* **2006**, *4*, 123−136.

(4) Tender, L. M.; Reimers, C. E.; Stecher, H. A., III; Holmes, D. E.; Bond, D. R.; Lowy, D. A.; Pilobello, K.; Fertig, S. J.; Lovley, D. R. Harnessing microbially generated power on the seafloor. *Nat. Biotechnol.* **2002**, *20*, 821−825.

(5) Reimers, C. E.; Stecher, H. A., III; Westall, J. C.; Alleau, Y.; Howell, K. A.; Soule, L.; White, H. K.; Girguis, P. R. Substrate degradation kinetics, microbial diversity, and current efficiency of microbial fuel cells supplied with marine plankton. *Appl. Environ. Microbiol.* **2007**, in press.

(6) Froelich, P. N.; Klinkhammer, G. P.; Bender, M. L.; Luedtke, N. A.; Heath, G. R.; Cullen, D.; Dauphin, P.; Hammond, D. E.; Hartman, B.; Maynard, V. Early oxidation of organic matter in pelagic sediments of the eastern equatorial Atlantic: Suboxic diagenesis. *Geochim. Cosmochim. Acta* **1979**, *43*, 1075−1090.

(7) Burdige, D. J. *Geochemistry of Marine Sediments*; Princeton University Press: Princeton, NJ, 2006.

(8) Finkelstein, D. A.; Tender, L. M.; Zeikus, J. G. Effect of electrode potential on electrode-reducing microbiota. *Environ. Sci. Technol.* **2006**, *40*, 6990−6995.
(9) He, Z.; Haibo, S.; Angenent, L. T. Increased power production from a sediment microbial fuel cell with a rotating cathode. *Biosens. Bioelectron.* **2007**, *22*, 3252−3255.
(10) Holmes, D. E.; Bond, D. R.; O'Neill, R. A.; Reimers, C. E.; Tender, L. R.; Lovley, D. R. Microbial communities associated with electrodes harvesting electricity from a variety of aquatic sediments. *Microb. Ecol.* **2004**, *48*, 178−190.
(11) Lowy, D. A.; Tender, L. M.; Zeikus, J. G.; Park, D. H.; Lovley, D. R. Harvesting energy from the marine sediment−water interface. II. Kinetic activity of anode materials. *Biosens. Bioelectron.* **2006**, *21*, 2058−2063.
(12) Ryckelynck, N.; Stecher, H. A., III; Reimers, C. E. Understanding the anodic mechanism of a seafloor fuel cell: Interactions between geochemistry and microbial activity. *Biogeochemistry* **2005**, *76*, 113−139.
(13) Farzaneh, R.; Richard, T. L.; Brennan, R. A.; Logan, B. E. Substrate-enhanced microbial fuel cells for improved power generation from sediment-based systems. *Environ. Sci. Technol.* **2007**, *41*, 4053−4058.
(14) Cheng, S.; Liu, H.; Logan, B. E. Increased power generation in a continuous flow MFC with advective flow through the porous anode and reduced electrode spacing. *Environ. Sci. Technol.* **2006**, *40*, 2426−2432.
(15) Rabaey, K.; Clauwaert, P.; Aelterman, P.; Verstraete, W. Tubular microbial fuel cells for efficient electricity generation. *Environ. Sci. Technol.* **2005**, *39*, 8077−8082.
(16) Jang, J. K.; Pham, T. H.; Chang, I. S.; Kang, K. H.; Moon, H.; Cho, K. S.; Kim, B. H. Construction and operation of a novel mediator- and membrane-less microbial fuel cell. *Process Biochem. (Oxford, U.K.)* **2004**, *39*, 1007−1012.
(17) He, Z.; Minteer, S. D.; Angenent, L. T. Electricity generation from artificial wastewater using an upflow microbial fuel cell. *Environ. Sci. Technol.* **2005**, *39*, 5262−5267.
(18) Moon, H.; Chang, I. S.; Kim, B. H. Continuous electricity production from artificial wastewater using a mediator-less microbial fuel cell. *Bioresour. Technol.* **2006**, *97*, 621−627.
(19) Logan, B. E.; Hamelers, B.; Rozendal, R.; Schroder, U.; Keller, J.; Freguia, S.; Aelterman, P.; Verstraete, W.; Rabaey, K. Microbial fuel cells: Methodology and technology. *Environ. Sci. Technol.* **2006**, *40*, 5181−5192.
(20) Hasvold, O.; Henriksen, H.; Melvaer, E.; Citi, G.; Johansen, B. O.; Kjonigsen, T.; Galetti, R. Sea-water battery for subsea control systems. *J. Power Sources* **1997**, *65*, 253−261.
(21) Logan, B. E.; Cheng, S.; Watson, V.; Estadt, G. Graphite fiber brush anodes for increased power production in air-cathode microbial fuel cells. *Environ. Sci. Technol.* **2007**, *41*, 3341−3346.
(22) Cline, J. D. Spectrophotometric determination of hydrogen sulfide in natural waters. *Limnol. Oceanogr.* **1969**, *14*, 454−458.
(23) Solorzano, L. Determination of ammonia in natural waters by the phenolhypochlorite method. *Limnol. Oceanogr.* **1969**, *14*, 799−801.
(24) Johnson, K. M.; King, A. E.; Sieburth, J. M. Coulometric DIC analyses for marine studies: An introduction. *Mar. Chem.* **1985**, *16*, 61−82.
(25) Aelterman, P.; Rabaey, K.; Pham, H. T.; Boon, N.; Verstraete, W. Continuous electricity generation at high voltages and currents using stacked microbial fuel cells. *Environ. Sci. Technol.* **2006**, *40*, 3388−3394.
(26) Larminie, J.; Dicks, A. *Fuel Cell Systems Explained*, 1st ed.; John Wiley and Sons Ltd.: New York, 2000.
(27) Pilson, M. E. Q. *An Introduction to Chemistry of the Sea*; Prentice Hall: New York, 1998.
(28) Dumbauld, B. R.; Armstrong, D. A.; Feldman, K. L. Life history of two sympatric Thalassinidean shrimps, *Neotrypaea californiensis* and *Upogebia pugettensis*, with implications for oyster culture. *J. Crustacean Biol.* **1996**, *16*, 689−708.
(29) Rabaey, K.; Van de Sompel, K.; Maignien, L.; Boon, N.; Aelterman, P.; Clauwaert, P.; De Schamphelaire, L.; Pham, H. T.; Vermeulen, J.; Verhaege, M.; Lens, P.; Verstraete, W. Microbial fuel cells for sulfide removal. *Environ. Sci. Technol.* **2006**, *40*, 5218−5224.
(30) Huettel, M.; Ziebis, W.; Forster, S.; Luther, G. W. Advective transport affecting metal and nutrient distributions and interfacial fluxes in permeable sediments. *Geochim. Cosmochim. Acta* **1998**, *62*, 613−631.
(31) Elderfield, H.; Schultz, A. Mid-ocean ridge hydrothermal fluxes and the chemical composition of the ocean. *Annu. Rev. Earth Planet. Sci.* **1996**, *24*, 191−224.
(32) Torres, M. E.; McManus, J.; Hammond, D. E.; de Angelis, M. A.; Heeschen, K. U.; Colbert, S. L.; Tryon, M. D.; Brown, K. M.; Suess, E. Fluid and chemical fluxes in and out of sediments hosting methane hydrate deposits on Hydrate Ridge, OR. I. Hydrological provinces. *Earth Planet. Sci. Lett.* **2002**, *201*, 525−540.

Received for review July 13, 2007. Revised manuscript received August 30, 2007. Accepted September 4, 2007.

ES071740B